is essentially the same estimated by experiments and other calculations for other α-diimine complexes.[9] It is certainly a significant amount for Fe(II) but does not correspond to a *major* role for resonance structures with multiple Fe–N bonds.

It is interesting to note that the prediction of Figure 2, on the face of it, is that the electron added upon *reduction* of $FeTIM(NCS)_2$ would go into a mainly TIM C–N π^* rather than into an Fe $d\pi$ orbital, thus forming an Fe(II)–TIM radical anion complex. Although we know of no well-characterized iron complexes of this sort, a number of "Ni(I)" complexes of conjugated macrocyclic ligands have been shown experimentally to contain in fact Ni(II) and ligand radical anions.[19]

(19) Gagné, R. R.; Ingle, D. M. *J. Am. Chem. Soc.* **1980**, *102*, 1444 and references therein.

On the basis of these results, one is led to speculate that the HOMO's of $FeTIM(MeOH)_2^{2+}$ might indeed have considerable ligand character, through interaction of the Fe $d\pi$ and oxygen-localized MeOH lone-pair orbitals. A calculation on $Fe(N_2C_2H_4)_2(MeOH)_2$ itself would be worthwhile due to its catalytic function. We hope eventually to deal with the subtle question of how TIM, as opposed to other neutral macrocycles which set up strong ligand fields, conveys special properties to these systems.

Acknowledgment. We are grateful to E. O. Fey, R. R. Gagné, M. Maroney, and L. Noodleman for discussions and communication of results. We thank the National Science Foundation for support.

Registry No. **2**, 76705-28-7; 2^+, 76705-29-8; 3^+, 76705-30-1; $N_2C_2H_4$, 40079-19-4; NCS^-, 302-04-5; $FeTIM(NCS)_2$, 69765-88-4.

Contribution from the Department of Chemistry, Rutgers University, New Brunswick, New Jersey 08903

Intercalation Compounds of FeOCl: Systematics of Nitrogen-Containing Lewis Base Intercalants

ROLFE H. HERBER* and YONEZO MAEDA

Received August 5, 1980

Ten nitrogen-containing Lewis base intercalates of iron(III) oxychloride, $FeOCl(G)_n$, have been prepared and characterized by elemental analysis, powder pattern X-ray diffraction, and ^{57}Fe Mössbauer and Fourier transform infrared spectroscopies. The unit cell *b*-axis expansion confirms the location of the "guest" molecule within the van der Waals layer of the FeOCl lattice, and the magnitude of this expansion provides information concerning the orientation of the intercalant within this layer. The magnetic ordering temperature of FeOCl (90 ± 2 K) is depressed in the intercalates to temperatures below ~78 K. The magnitude of the magnetic hyperfine field in the low-temperature limit (4.2 K) is about 2% larger in the pyridine, ammonia, 2-picoline, and butylamine intercalates than it is in unintercalated FeOCl. The sign of the EFG tensor at the iron atom is a function of stoichiometry rather than dependent on the bonding and structural parameters of the intercalant per se. The Fourier transform infrared spectra of several of the intercalates have been examined in detail and show that a number of fundamental modes—especially those involving ring-breathing modes of the "guest" species—are strongly suppressed in the intercalate.

Introduction

FeOCl is a layered compound belonging to the orthorhombic space group *Pmnm* (D_{2h}^{13}) with 2 formula units per unit cell.[1,2] The crystal structure consists of a stack of double sheets of *cis*-$FeCl_2O_4$ octahedra, linked together with shared edges. The unit cell dimensions are $a = 3.780$, $b = 7.917$, and $c = 3.302$ Å. Of particular significance is the fact that the chlorine atoms lie on a plane which defines the edge of each layer, and the bonding across these chlorine atom planes is assumed to be of the van der Waals type. The van der Waals interaction is easily disrupted, and the intercalation of a wide variety of amine bases has been observed to occur under relatively mild conditions.[3,4] The orientation of the intercalated molecular species has been the subject of extensive study, and the *b*-axis expansion of the unit cell as derived from X-ray powder pattern data has been used to elucidate the steric relationships between the guest molecule and the host lattice.

A large number of different Lewis bases including ammonia,[3] pyridine and pyridine derivatives,[5–8] phosphine, and phosphite[9] have been successfully intercalated into FeOCl. It has been observed that, while nonstoichiometric iron(III) oxychloride is capable of intercalating a large number of molecules having Lewis base character, studies of stoichiometric FeOCl base intercalates have so far focused on pyridine and its derivatives as "guest molecules". A lithium intercalate, $FeOClLi_x$ ($x = 0.50$), has been reported by Palvadeau et al.[4] The FeOCl intercalation of two cyclopentadienyl organometallic compounds has been reported by Halbert et al.[10]

In the present study, ten intercalation compounds in which nitrogen-containing Lewis bases are present as guest molecules (G) in an FeOCl host matrix have been prepared, and the hyperfine interactions, lattic dynamics, and vibrational spectra of the systems $FeOCl(G)_n$ are discussed in detail.

Experimental Section

(a) Sample Preparation. Iron(III) oxychloride was prepared from Fe_2O_3 and $FeCl_3$ by the usual sealed-tube technique discussed in the literature[6–8] and was characterized by colorimetric iron determination and X-ray powder patterns. The intercalates listed in Table I were obtained by soaking FeOCl in the amine base (if a liquid) or in the base dissolved in a suitable solvent. Careful attention was paid during

(1) Goldsztaub, S. *C. R. Hebd. Seances Acad. Sci.* **1934**, *198*, 667; *Bull. Soc. Fr. Mineral. Cristallogr.* **1935**, *58*, 6.
(2) Lind, M. D. *Acta Crystallogr., Sect. B* **1970**, *B26*, 1058.
(3) Hagenmuller, P.; Portier, J.; Barbe, B.; Bouclier, P. *Z. Anorg. Allg. Chem.* **1967**, *355*, 209.
(4) Palvadeau, P.; Coic, L.; Rouxel, J.; Portier, J. *Mater. Res. Bull.* **1978**, *13*, 221.
(5) Herber, R. H.; Maeda, Y. "Proceedings of the Conference on Nuclear and Electron Resonance Spectroscopies Applied to Materials Science"; Kaufmann, E. N., Shenoy, G. K., Eds.; North-Holland Publishing Co.: Amsterdam, in press.
(6) Kanamaru, F.; Yamanaka, S.; Koizumi, M.; Nagai, S. *Chem. Lett.* **1974**, 373.
(7) Kikkawa, S.; Kanamaru, F.; Koizumi, M. *Bull. Chem. Soc. Jpn.* **1979**, *52*, 963.
(8) Kanamaru, F.; Shimada, M.; Koizumi, M.; Takao, M. Takada, T. *J. Solid State Chem.* **1973**, *7*, 297.
(9) Herber, R. H.; Maeda, Y. *Inorg. Chem.* **1980**, *19*, 3411.
(10) Halbert, T. R.; Johnston, D. C.; McCandlish, L. E.; Thompson, A. H.; Scanton, J. R.; Dumesic, J. A. *Physica B+C* **1980**, *99B+C*, 128. T. R. Halbert and J. R. Scanlon, *Mater. Res. Bull.* **1979**, *14*, 415.

0020-1669/81/1320-1409$01.25/0

Table I. Preparative Conditions and pK_a for $FeOCl(G)_n$ Intercalates

intercalates	n	G	reacn temp, °C	reacn time	solvent	pK_a (at 20 °C)
pyridine	1/3	py	80	7 d		5.17
NH_3	3/4	amm	−80	45 m		9.2
isopropylamine	1/3	isopropyl	24	11 h		11.54
2-picoline	1/4	pic	50	14 d		5.97
butylamine	1/4	butyl	24	45 m		10.7
diazabicyclo[2.2.2]octane	1/6	octa	50	17 d	EtOH	8.19
imidazole	1/4	imid	50	14 d	EtOH	7.20
quinuclidine	1/6	quin	50	7 d	EtOH	10.65
2,6-lutidine	1/6	lut	50	14 d		6.58
dodecylamine	1/6	dodec	35	60 m		10.63

Table II. Analytical Data for the Intercalates[a]

intercalates	C	H	N	Cl	Fe
$(py)_{1/3}$	15.20	1.32	3.49	26.22	41.65
	(14.96)	(1.25)	(3.49)	(26.52)	(41.78)
$(NH_3)_{3/4}$		1.50	8.85	30.46	46.90
		(1.87)	(8.75)	(29.53)	(46.52)
$(isopropyl)_{1/3}$					43.89
					(43.98)
$(2\text{-pic})_{1/4}$	12.17	1.58	2.38	25.65	41.18
	(13.79)	(1.34)	(2.68)	(27.15)	(42.78)
$(butyl)_{1/4}\cdot{}^1/_8\,EtOH$[b]	11.30	2.68	2.70	27.57	43.30
	(11.62)	(2.64)	(2.71)	(27.44)	(43.22)
$(octa)_{1/6}\cdot{}^1/_3 H_2O$[c]	8.48	2.05	3.32	27.14	41.02
	(9.09)	(2.02)	(3.54)	(26.86)	(42.32)
$(imid)_{1/4}\cdot{}^1/_2 H_2O$	6.31	1.40	4.41	25.47	43.36
	(6.75)	(1.50)	(5.25)	(26.59)	(41.89)
$(quin)_{1/6}$	11.00	2.12	1.67	29.41	43.29
	(11.13)	(1.72)	(1.85)	(28.18)	(44.39)
$(lut)_{1/6}$	11.21	1.91	1.83	23.35	45.09
	(11.19)	(1.20)	(1.86)	(28.33)	(44.63)
$(dodec)_{1/6}$					39.16
					(40.42)

[a] The calculated values for the indicated stoichiometries are in parentheses and are based on elemental analyses (Galbraith) except for iron, which was determined colorimetrically in this study. [b] The presence of ethanol in this intercalate presumably arises from the washing procedure. [c] H_2O found in this intercalate comes from the presence of H_2O in the Lewis base as used.

the preparation of both FeOCl and its intercalation compounds to the rigorous exclusion of moisture by use of an inert-atmosphere glovebox to carry out all sample manipulations. The experimental conditions for preparation of the compounds and analytical data are summarized in Tables I and II. The presence of ethanol in the butyl intercalate and of water in the octa and imid intercalates was inferred from the analytical results. At the end of the reaction period, the reaction mixture was filtered through sintered glass, and the solid product was washed with absolute alcohol, dried in vacuo, and stored under nitrogen. As Hagenmuller et al.[3] and others have pointed out, the stoichiometry of the FeOCl guest is strongly dependent on the steric requirements of the Lewis base "guest" atom. Powder X-ray patterns of all intercalates show the absence of unreacted (unintercalated) FeOCl. Completion of the intercalation was inferred from the time dependence of the X-ray diffraction powder patterns, especially of the reflections related to the *b* and *c* axes of the unit cell. The reflection lines due to the (010) and (020) planes of the intercalates were used to calculate the length of the *b* axis and are listed in Table IV. The *b*-axis length of FeOCl(dodec) was not calculated since it did not show any systematic reflections which could be indexed.

(b) Spectroscopy. Infrared spectra were obtained with use of a Perkin-Elmer Model 283 spectrophotometer on ~0.5% by weight KBr pellets. Mössbauer spectra were obtained as described earlier.[11-13] All isomer shifts (IS) are reported with respect to the centroid of the room-temperature spectrum of metallic iron. Data reduction was effected with use of a matrix inversion least-squares routine on the Rutgers University IBM 370/168 computer. Since the temperature dependence of the recoil-free fraction can be estimated for a thin absorber from the temperature dependence of the area under the resonance curve (vide infra), thin absorbers containing ~3 mg of Fe/cm^2 were used in this study. In the usual procedure, the sample interclate was mixed with 10 mg of SiO_2 and 80 mg of boron nitride to facilitate handling and to optimize random crystallite orientation and mounted between high-purity aluminum foils in a copper sample holder.

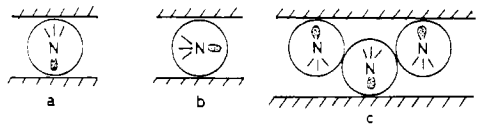

Figure 1. Three possible orientations of pyridine and related Lewis base intercalants within the FeOCl layer lattice. The van der Waals gap into which the "guest" molecules are inserted are defined by the chlorine atoms of the matrix.

Results and Discussion

(a) Lattice Parameters of Intercalated FeOCl. The X-ray powder patterns of these solids show that while the *a*- and *c*-axis parameters do not change significantly when FeOCl is intercalated with a "guest" molecule, the *b*-axis parameter undergoes a large increase. There are several possible orientations which a noncubic symmetry intercalant molecule can adopt with respect to the symmetry of the lattice. In particular, it is of interest to ascertain the orientation of the nitrogen lone-pair electrons with respect to the van der Waals layer, since any discussion of the "guest–host" chemical interaction must take this question into account.

The interlayer spacing, which amounts to 7.91 Å for FeOCl, increases during the reaction with NH_3. In the intercalate $FeOCl(NH_3)_{3/4}$ the *b*-axis unit cell dimension is 11.33 Å, and this increase of 3.42 Å in the *b* unit cell parameter is larger than the covalent diameter of NH_3 itself (2.52 Å). In the intercalate $FeOCl(NH_3)_{1/2}$, the *b*-axis unit cell dimension is 10.37 Å; that is, the expansion is just that corresponding to the covalent diameter of the "guest" molecule. Several structural models have been proposed to account for the orientation of the Lewis base "guest" molecules in the FeOCl lattice, and these are schematically summarized in Figure 1. In Figure 1a, the lone-pair electrons are directed parallel to the *b* axis, that is, orthogonal to the van der Waals plane. Since the C_{3v} axis of NH_3 is less than 2 Å, this orientation does not readily account for the observed *b*-axis expansion in $FeOCl(NH_3)_{3/4}$. The orientation shown in Figure 1b is one in which the nitrogen atom lone pair is oriented to the van der Waals plane. This orientation does not readily account for the observed interlayer spacing for the $FeOCl(NH_3)_{3/4}$ intercalate nor for the observation that the *b*-axis expansion in this compound is similar to that observed in FeOCl(isopropyl)$_{1/3}$ and FeOCl(butyl)$_{1/4}$. Thus, a monolayer chain of the type shown in Figure 1a,b can probably be ruled out for these compounds. A staggered guest molecular arrangement of the type shown in Figure 1c, in which repulsion between hydrogen atoms of adjacent NH_3 molecules is minimized,

(11) Herber, R. H.; Maeda, Y. *Physica B+C* **1980**, *99B+C*, 352.
(12) Rein, A. J.; Herber, R. H. *J. Chem. Phys.* **1975**, *63*, 1021.
(13) (a) Katada, M.; Herber, R. H. *J. Solid State Chem.* **1980**, *33*, 361. (b) Calculated from covalent radii; see, for example: Huheey, J. E. "Inorganic Chemistry"; Harper and Row: New York, 1972; Table 5.1.

Table III. Mössbauer Parameters of FeOCl Intercalation Compounds[a]

intercalant	QS		IS		H_i, kOe[c]
	78 K[b]	300 K	78 K[b]	300 K	
FeOCl	0.929 ± 0.010	0.906 ± 0.010	0.511 ± 0.008	0.389 ± 0.006	−432 ± 1
$(py)_{1/3}$	1.252 ± 0.022	0.670 ± 0.008	0.477 ± 0.030	0.461 ± 0.076	+444 ± 1
$(NH_3)_{3/4}$	0.986 ± 0.008	0.780 ± 0.003	0.480 ± 0.024	0.409 ± 0.018	+443 ± 1
$(isopropyl)_{1/3}$	1.184 ± 0.014	0.775 ± 0.004	0.523 ± 0.052	0.453 ± 0.054	
$(2\text{-pic})_{1/4}$	1.146 ± 0.015	0.935 ± 0.001	0.503 ± 0.017	0.404 ± 0.044	−443 ± 1
$(butyl)_{1/4}$	1.051 ± 0.005	0.805 ± 0.003	0.504 ± 0.023	0.410 ± 0.034	−437 ± 1
$(octa)_{1/6}$	1.184 ± 0.013	0.689 ± 0.008	0.510 ± 0.042	0.454 ± 0.060	
$(imid)_{1/4}$	1.191 ± 0.017	0.816 ± 0.016	0.501 ± 0.043	0.422 ± 0.043	
$(quin)_{1/6}$	1.210 ± 0.019	0.754 ± 0.014	0.517 ± 0.064	0.465 ± 0.072	
$(2,6\text{-lut})_{1/6}$	1.158 ± 0.020	0.765 ± 0.022	0.514 ± 0.078	0.454 ± 0.090	
$(dodec)_{1/6}$	1.016 ± 0.016	0.929 ± 0.10	0.486 ± 0.034	0.370 ± 0.030	

[a] In mm s^{-1} (except for H_i). [b] In those cases where the magnetic ordering temperature is above 78 K, the indicated value is that obtained by appropriate extrapolation of higher temperature data. [c] The sign preceding H_i is that of V_{zz} deduced from the magnetic spectra.

Table IV. Temperature Dependence of Mössbauer Parameters, Lattice Temperatures, and *b*-Axis Spacings for FeOCl Intercalation Compounds

intercalant	$-d(IS)/dT \times 10^4$, mm s^{-1} K^{-1}	int.	cc	M_{eff}, amu	Θ_M', K	$-d \ln A/dT \times 10^3$, K^{-1}	cc	Θ_M, K	temp range, K	*b*, Å
FeOCl	5.291	0.517	0.996	79 ± 1	290.6	1.185	0.988	341 ± 4	97.5–303	7.91
$(py)_{1/3}$	4.692	0.600	0.998	89 ± 1	160 ± 5	3.412	0.998	200 ± 6	>225	13.45
$(NH_3)_{3/4}$	5.081	0.563	0.992	82 ± 1	218 ± 7	1.994	0.998	261 ± 8	>150	11.33
$(isopropyl)_{1/3}$	3.161	0.554	0.970	132 ± 1	155 ± 5	2.466	0.994	235 ± 7	>150	11.90
$(2\text{ pic})_{1/4}$	3.685	0.532	0.991	113 ± 1	168 ± 5	2.224	0.996	247 ± 8	100–225	13.52
	5.917	0.582	0.999	70 ± 1	213 ± 7	3.204	0.999	206 ± 7	>250	
$(butyl)_{1/4}$	4.829	0.544	0.993	86 ± 1	171 ± 5	3.084	0.999	210 ± 7	>125	11.71
$(octa)_{1/6}$	4.363	0.587	0.994	96 ± 1	170 ± 5	2.807	0.998	220 ± 7	>225	13.06
$(imid)_{1/4}$	4.536	0.559	0.996	92 ± 1	175 ± 5	2.750	0.997	222 ± 7	>150	13.16
$(quin)_{1/6}$	4.603	0.597	0.953	91 ± 1	172 ± 5	2.908	0.998	216 ± 7	200–300	13.36
$(2,6\text{-lut})_{1/6}$	4.314	0.577	0.980	97 ± 1	162 ± 5	3.064	0.998	211 ± 7	>200	14.80
$(dodec)_{1/6}$	6.427	0.552	0.993	65 ± 1	169 ± 5	4.196	0.999	180 ± 6	150–250	
						7.514	0.999	135 ± 4	>250	

would account for the experimentally observed data but cannot be unambiguously demonstrated on the basis of powder pattern X-ray data alone.

In the intercalate $FeOCl(py)_{1/3}$ the *b*-axis unit cell expansion is 5.54 Å, in good agreement with that observed in the intercalate formed with 4-(dimethylamino)pyridine (DMAP) in which the corresponding value is 5.50 Å. Since the end-to-end dimension of the latter molecule is ~6.9 Å, it is clear that, for these relatively large intercalants, the molecular orientation cannot correspond to that shown in Figure 1a. It is likely that the major interaction between the Lewis base and the matrix is one which the lone-pair electrons can overlap significantly with a vacant d orbital of Fe(III), resulting in a nonorthogonal orientation of the major molecule axis relative to the unit cell axes of the host matrix. The near identity of the *b*-axis expansion in $FeOCl(py)_{1/3}$ and $FeOCl(DMAP)_{1/6}$ relative to the unintercalated matrix is again consistent with the model shown in Figure 1c, but with a tilt of the major guest molecular axis from the perpendicular, as needed to accommodate the guest species within the host matrix.

(b) Acid Dissociation Constants (pK_a). The pK_a values of the intercalant species are included in the data summarized in Table I. As an approximate rule, it can be inferred from the presently available data that a necessary (but not sufficient) condition for forming the FeOCl intercalate of these molecules under the relatively mild conditions detailed above is that the pK_a must be larger than ~5. Variations of solvent, as well as other experimental conditions, will modify this requirement. Moreover, the basicity of the lone-pair electrons is strongly dependent on the nature and position of the ring substituents in the case of pyridine derivatives, and numerous interrelated factors influencing the availability of the lone-pair electrons must be taken into account. Nonetheless, the observation is valid that most nitrogen-containing bases with $pK_a \geq 5$ can be successfully intercalated into FeOCl. Isoquinoline (pK_a = 5.3) and piperidine (pK_a = 11.28) appear to be exceptions to the general rule. On the other hand, all efforts to date to intercalate quinoline (pK_a = 4.88), aniline (pK_a = 4.58), 1,10-phenanthroline (pK_a = 4.65), bipyridine (pK_a = 4.19), and pyrimidine (pK_a = 1.23) into FeOCl have been unsuccessful.

(c) Mössbauer Spectra. The data extracted from the ^{57}Fe Mössbauer spectra of the various $FeOCl(G)_n$ intercalates examined in the present study are summarized in Tables III and IV. Before considering the temperature dependence of the hyperfine interaction parameters, which will be discussed more fully below, it is appropriate to examine the temperature dependence of the recoil-free fraction and its relationship to the lattice dynamical properties of the intercalate systems. It has already been noted that, when the limiting composition is reached during the intercalation process, the X-ray powder patterns reveal unambiguously the disappearance of the scattering maxima characteristic of neat FeOCl and the appearance of a powder pattern which can be understood on the basis of an expansion of *every* layer in the direction of the *b* axis of the unit cell. This observation is consistent with the formation of a "stage 1" compound in which every van der Waals layer includes a regular array of "guest" molecules. In view of the foregoing and the experimentally observed limiting stoichiometry in which $^1/_6 \leq n \leq {}^3/_4$, it might be expected that not all of the iron atoms in the intercalate $FeOCl(G)_n$ are chemically (and structurally) identical and hence that the Mössbauer spectra might show resonances characteristic of each kind of iron atom in the structure. This expectation has not been met in the ^{57}Fe resonance spectra of the intercalates at temperatures well above the magnetic ordering temperature. In this regime, all the spectra could be fitted with a single doublet pair. If—on the Mössbauer time scale—there are

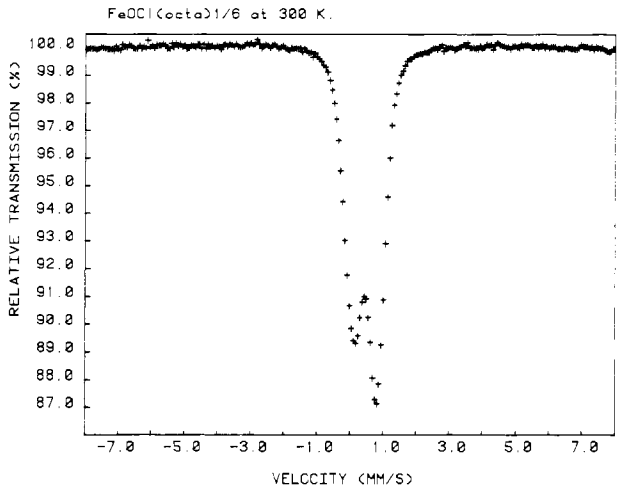

Figure 2. ^{57}Fe Mössbauer effect spectrum of the 1,4-diazabicyclo-[2.2.2]octane [octa] intercalate of FeOCl at 300 K.

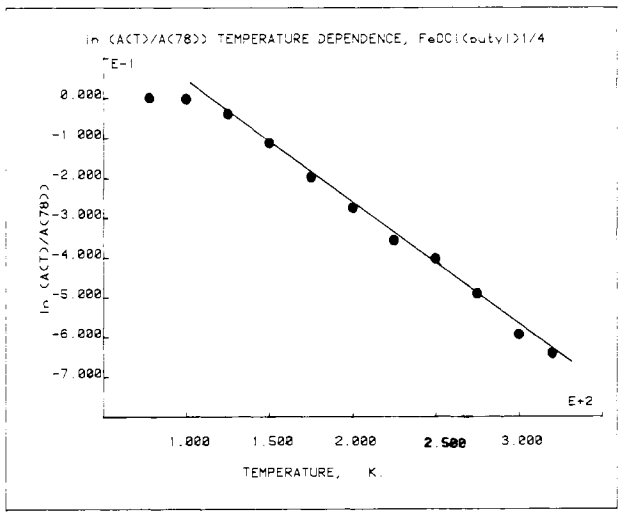

Figure 3. Temperature dependence of the normalized ln (area) parameter for the *n*-butylamine intercalate of FeOCl. The straight line represents a least-squares fit to the data for T in the range $125 \leq T \leq 320$ K.

indeed differences in the electronic environments of the several iron atoms in the intercalate structure, the spectroscopic resolution is insufficient to permit separation of the individual components from the spectral data. Thus, the following data analysis is based on a fitting of the resonance spectra in terms of a single doublet. A typical spectrum is shown in Figure 2.

At temperatures well above the magnetic ordering temperature, the temperature dependence of the area under the resonance curve can be used to estimate a "lattice temperature", Θ_M, based on the thermal motion of the Mössbauer-active atom. The temperature dependence of the area under the resonance curve (suitably normalized; in the present case to the 78 K datum) for a typical intercalate—FeOCl(butyl)$_{1/4}$—is shown in Figure 3. The data above ~100 K are well fit by a linear regression, and there is no evidence from these results of a first-order phase transition in the range $\sim 100 \leq T \leq 320$ K. As noted previously,[11] in the case of ^{57}Fe Mössbauer data, two "lattice temperatures" can be calculated from such data. Using a Debye model for the solid and assuming that the appropriate mass of the probe atom corresponds to the free-atom value lead to a temperature dependence of the recoil-free fraction, f, given by eq 1 in which E_R

$$\mathrm{d} \ln f/\mathrm{d}T = -6E_R/k_B\Theta_M^2 \quad (1)$$

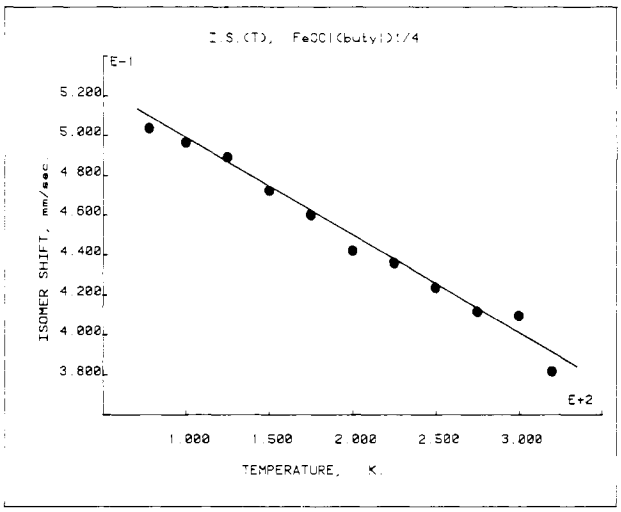

Figure 4. Temperature dependence of the isomer shift parameter for the *n*-butylamine intercalate of FeOCl. The straight line represents a linear least-squares fit to the data.

is the recoil energy after gamma ray emission and k_B is Boltzmann's constant. Equation 1 can be replaced for a thin absorber by the temperature dependence of the area under the resonance curve (appropriately normalized) and finally yields a relationship of the form

$$\Theta_M = \frac{E_\gamma}{c}\left[\frac{-3}{M_{\mathrm{eff}}k_B \mathrm{d} \ln [A(T)/A(78)]/\mathrm{d}T}\right]^{1/2} \quad (2)$$

For ^{57}Fe, this equation reduces to eq 3. A limitation of this

$$\Theta_M = 11.659\left[\frac{-\mathrm{d} \ln [A(T)/A(78)]}{\mathrm{d}T}\right]^{1/2} \quad (3)$$

approach is that, when the Mössbauer-active atom is incorporated in the solid by largely covalent bonding forces, the appropriate mass needed to describe its motional behavior may be significantly larger than the atomic mass, and thus the free-atom value (56.95 for Fe) must be replaced by an effective vibrating mass. This effective mass description has been especially useful in the description of molecular solids such as the organometallic compounds of iron[14] and tin.[12,15] In the case of ^{57}Fe spectroscopy, due to the lighter mass of the Mössbauer atom and the narrower line widths, as compared to the 23.87-keV resonance in ^{119}Sn, the effective vibrating mass can frequently be estimated with considerable accuracy from the second-order Doppler shift (the temperature dependence of the isomer shift parameter) and is given by eq 4. Using this value for M_{eff} in (2) leads to a modified lattice

$$M_{\mathrm{eff}} = -4.1684 \times 10^{-2}[\mathrm{d(IS)}/\mathrm{d}T]^{-1} \quad (4)$$

temperature (eq 5).

$$\Theta_M' = 4.3202 \times 10^2\left[\frac{\mathrm{d(IS)}/\mathrm{d}T}{\mathrm{d} \ln [A(T)/A(78)]/\mathrm{d}T}\right]^{1/2} \quad (5)$$

In contrast to the ln A temperature-dependence data which are well fit by a linear regression above ~100 K, the isomer shift data for a number of the intercalates examined in this study show a discontinuity in the temperature dependence at ~200 K. A typical data set—again for the FeOCl(butyl)$_{1/4}$ intercalate—is shown in Figure 4. The origin of this discontinuity in IS(T) will be discussed more fully below. In

(14) Hazony, Y.; Herber, R. H. *J. Phys.* **1974**, *66*, 131.
(15) Herber, R. H.; Leahy, M. F. *J. Chem. Phys.* **1977**, *67*, 2718.

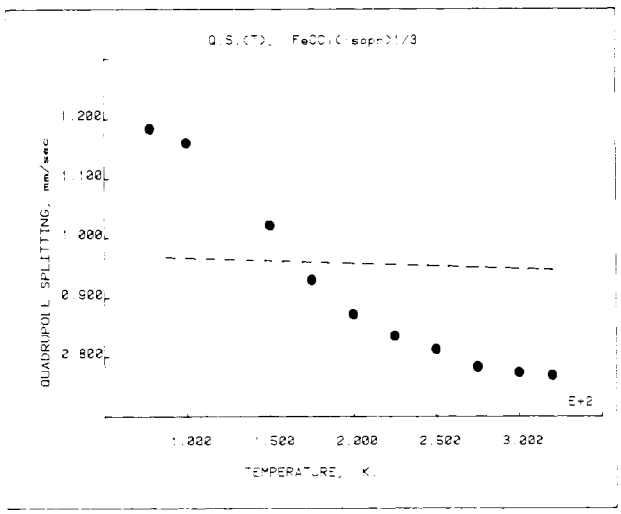

Figure 5. Temperature dependence of the quadrupole splitting parameter for the isopropylamine intercalate of FeOCl. The dashed line represents the comparison data for unintercalated FeOCl over the same temperature range. The origin of the sigmoid character of the QS data for the amine intercalate is discussed in the text.

order to estimate M_{eff}, only the data above the discontinuity have been utilized in the application of eq 4. The values of Θ_M calculated from eq 3 and Θ_M' calculated from eq 5 are summarized in Table IV, from which it is seen that M_{eff} is substantially larger than the free-atom value, and hence, generally $\Theta_M' < \Theta_M$ in consonance with the covalency of the iron atom bonding in the matrix. For most of the intercalates examined in this study, Θ_M'/Θ_M is approximately 0.80 ± 0.03, the exceptions being the isopropyl amine (0.66), the picoline (0.67), and the dodecylamine (0.94) compounds, as noted in the table. The significance in these data lie in the conclusion that the insertion of "guest" molecules into the van der Waals layer of the FeOCl structure and the concomitant significant *b*-axis expansion of the unit cell does not significantly effect the degree of covalency of the iron atom–nearest-neighbor interaction in the solid.

As we have already noted in an earlier study[11] of neat FeOCl, the temperature dependence of the quadrupole splitting hyperfine interaction parameter is very small, amounting to $\sim 1.0 \times 10^{-4}$ mm s^{-1} deg^{-1}, and is moderately well fitted by a linear regression in the temperature interval $100 \leq T \leq 320$ K. By contrast, most of the FeOCl intercalates examined in the present study show a nonlinear temperature dependence of the quadrupole hyperfine interaction. In some cases [e.g., FeOCl(butyl)$_{1/4}$], the low-temperature region and the high-temperature region individually evidence a nearly linear temperature dependence, with a recognizable discontinuity in the slope at ~190 K. In others [e.g., FeOCl(isopropyl)$_{1/3}$], the QS(T) behavior is significantly more sigmoid in character, with a relatively gradual transition from the low-temperature region dependence to that observed near the high-temperature limit. A typical QS(T) data set for the latter intercalation compound is summarized graphically in Figure 5.

The above observations relating to the temperature dependence of the quadrupole splitting hyperfine interaction parameter have been accounted for previously[9] by a model which envisions the behavior of the intercalates in the low-temperature region as that corresponding to a three-dimensional solid and in the high-temperature region as that corresponding to a quasi-two-dimensional solid. Since, as noted above, the transition between the two regimes is not sharp, it has so far not been possible to relate the onset of the high-temperature region behavior to specific structural, steric, or bonding properties of the intercalant. From the sigmoid shape of the QS(T) curve it may be inferred that the lattice energy across

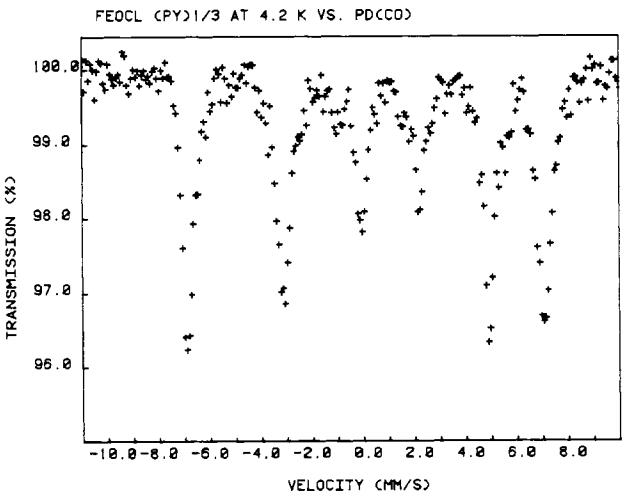

Figure 6. ^{57}Fe Mössbauer effect spectrum of the pyridine intercalate of FeOCl at liquid-helium temperature. Both the sign of V_{zz} (+) and the magnitude of the magnetic hyperfine field at the iron nucleus (444 ± 1 kOe) can be extracted from these data.

the van der Waals layer in the intercalates is on the order of 0.4–0.6 kcal mol^{-1}. Finally, it is appropriate to note, in this context, that the absolute value of the quadrupole hyperfine interaction in the intercalates is larger than that observed for the Fe(III) resonance in neat FeOCl at low temperatures and falls to a smaller value at high temperatures. This observation can be understood on the basis of the *b*-axis expansion in the intercalates: The constraints imposed on the bond angles of the (distorted) octahedral environment around each iron atom in the unintercalated matrix due to the chlorine–chlorine interactions across the van der Waals layer are relaxed in the intercalate.

When the temperature is increased from the low-temperature to the high-temperature region, the absence of direct Cl–Cl interactions permits a more facile change in the bond angles between iron and its nearest neighbors, resulting in a larger change in the EFG tensor at the iron atom between the two temperature regimes.

(d) Sign of the EFG Tensor and H_{int}. Due to the presence of a resolvable quadrupole hyperfine interaction and the existence of a readily accessible magnetic ordering temperature, it is possible to determine the sign of the EFG tensor from Mössbauer spectral data obtained at $T < T_N$. The magnetic ordering temperature of unintercalated FeOCl is 90 ± 2 K[11,16] and drops to a value below that of liquid-nitrogen temperature in the intercalates. At 4.2 K, the ^{57}Fe Mössbauer spectra consist of a six-line pattern, of which a typical example is shown in Figure 6. In several of the intercalates, the components of these low-temperature spectra are significantly broadened over those observed in neat FeOCl, indicative of the existence of several (slightly) different iron atoms and/or two or more magnetic hyperfine fields at the iron nuclei in the matrix of the intercalates. In those cases where no significant broadening is observed to occur, the magnitude of the magnetic hyperfine field at the iron nucleus, H_{int}, has been calculated from the position of the two "outside" lines of the six-line spectrum, and these values are included in the data summarized in Table III, from which it is noted that, in the intercalates, there is a small (~2–3%) increase in H_{int} over that observed in unintercalated FeOCl.

In addition, these 4.2 K spectra permit the evaluation of the sign of the EFG tensor, which is obtained from the relative

(16) Grant, R. W.; Wiedersich, H.; Housley, R. M.; Espinosa, G. P.; Artman, J. O. *Phys. Rev. B: Solid State* **1971**, *3B*, 678. Grant, R. W. *J. Appl. Phys.* **1971**, *42*, 1619.

Table V. Infrared Assignments and Intensities for $FeOCl(py)_{1/3}$ in KBr

ν, cm^{-1}	no.[a]	sym (C_{2v})	assignt	intens
405 s	16a,b	A_2, B_2	out of plane bending?	obscured
604 s	6a,b	A_1, B_1	sym ring breathing	strongly suppressed
703 vvs	11	B_2	out of plane bending	obsd
749 m	10a,b	A_2, B_2	out of plane bending	obsd
991 vs	1	A_1	sym ring expansion	strongly suppressed
1030 vs	12	A_1	sym ring expansion	strongly suppressed
1068 s	18a,b	A_1, B_1	axial expansion and H atom in-plane bend	strongly suppressed
1148 s	15, 9a	B_1	H scissor motion in-plane?	obscured
1217 s	3	B_1	rotational motion of H in-plane	w sh (supp?)
	9a,b	A_1, B_1		
1375 m	14	B_1	H scissor motion in-plane	w
1441 vs	19a,b	A_1, B_1	H scissor motion in-plane	obsd (br)
1482 s	19a,b	A_1, B_1	H scissor motion in-plane	obsd (br)
1572 m	8a,b	A_1, B_1	sym scissor motion in-plane	obscured
1583 vs	8a,b	A_1, B_1	sym scissor motion in-plane	obscured
1599 m				obscured
1872 m			comb. and overtones (8b + 16a, 1 + 3, 11 + 19a)	strongly suppressed
1923 m			comb. and overtones (3 + 2, 6a + 19a, 2 × 1, 6b + 19b)	strongly suppressed
1987 m				
2960 m				vw
3004 s				vw
3036 vs	20a,b	A_1, B_1	H deformation in-plane	strongly suppressed
3055 s	2, 7a,b, 13	A_1, B_1	comb. (2 × 8b)	strongly suppressed
3083 vs	20a,b	A_1, B_1	H deformation in-plane	strongly suppressed

[a] Reference 20.

Table VI. Infrared Assignments and Intensities for $FeOCl(imid)_{1/4}(H_2O)_{1/2}$

ν, cm^{-1}	no.[a]	sym (C_{2v})	assignt	intens
620 s	21	B_2	N–H out-of-plane bend	obsd
658 s	20	B_2	ring torsion	strongly suppressed
740 m	19 (?)	B_2	CH out-of-plane bend	suppressed?
760 s	18	B_2	CH out-of-plane bend	obsd (br)
827 m	9	A_1	ring expansion (axial)	strongly suppressed
841 s	9	A_1	ring expansion (axial)	strongly suppressed
934 s	16	B_1	CH bend or out of plane	strongly suppressed
1058 s	8	A_1	CH bend, scissor	shifted to 1045 cm^{-1} (?)
1145 m	7	A_1	NH bend	shifted to 1137 cm^{-1} (?)
1264 m	6	A_1	ring expansion	strongly suppressed
1324 m	14	B_1	CH in-plane def	strongly suppressed
1451 m	5	A_1	ring expansion	shifted to 1420 cm^{-1} (?)
2590 m				w sh
2692 m			(A) sym in-plane H str or (B) asym in-plane H str	w or suppressed
2785 m				sh
2934 m				obsd (br)
3030 m				suppressed
3125 m	10	B_1	asym in-plane H str	obsd (br)

[a] Reference 22.

separation of the 1,2 and 5,6 resonance maxima (numbering sequentially from lower to higher Doppler velocity). In $FeOCl(pic)_{1/4}$ and $FeOCl(butyl)_{1/4}$, the sign of V_{zz} is negative, as it is in unintercalated FeOCl. For $FeOCl(NH_3)_{3/4}$ and $FeOCl(py)_{1/3}$, this sign is positive. Whether or not there is a specific relationship between the sign of V_{zz} and the size or structure of the intercalant molecule has not yet been demonstrated. In fact, the presently available evidence suggests that stoichiometry, rather than structure per se, is decisive. For the intercalates $FeOCl(G)_n$, V_{zz} has been observed to be negative for $n \leq 1/4$ and positive for $n \geq 1/3$. A detailed, quantitative explanation for these observations is not yet at hand.

(e) Infrared Spectra. $FeOCl(py)_{1/3}$. The room-temperature Fourier transform infrared spectra of $FeOCl(py)_{1/3}$ in a KBr matrix (upper trace) and of neat pyridine (lower trace) are shown in Figure 7. In the upper trace, the strong absorptions at 500–540 (br) and 1640 cm^{-1}, as well as some weaker features lying between 1400–1500 cm^{-1}, are due to the FeOCl matrix. Most notable in a comparison of the two spectra are the observations that the out-of-plane bending modes of pyridine[17,18] at 703 and 749 cm^{-1} are clearly noted in the intercalate spectrum, while the symmetric ring expansion mode at 991 cm^{-1}, the alternant symmetric (A_1) ring expansion mode at 1030 cm^{-1} and the combination axial expansion and H-atom in-plane bend (A_1, B_1) at 1068 cm^{-1} are strongly suppressed in the intercalate spectrum. Similarly, the medium-strong combination and overtone bands at 1872 and 1923 cm^{-1}, as well as the very strong overtone band at 3083 cm^{-1}, are strongly suppressed in the $FeOCl(py)_{1/3}$ spectrum. A summary of the assignments of the vibrational modes of pyridine and the observations relating to the intercalate spectra is given in Table V in which the numbering system due to Wilson[19] and Kline and Turkevich[20] have been followed.

These observations indicate clearly that the orientation of the pyridine molecule is such that the plane of the ring is perpendicular to the chlorine atom planes which define the van der Waals layer. Within that restriction, two extremum

(17) Corrsin, L.; Fax, B. J.; Lord, R. C. *J. Chem. Phys.* **1953**, *21*, 1170.
(18) Lord, R. C.; Marston, A. L.; Miller, Foil A. *Spectrochim. Acta* **1957**, *9*, 113.
(19) Wilson, E. B. *Phys. Rev.* **1934**, *45*, 706.
(20) Kline, C. H., Jr.; Turkevich, J. *J. Chem. Phys.* **1944**, *12*, 300.

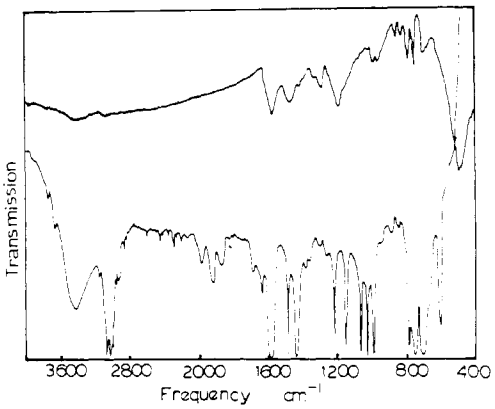

Figure 7. Fourier transform spectrum of $FeOCl(py)_{1/3}$ at room temperature (upper trace) and of pyridine (lower trace) over the range $4000 \geq \nu \geq 400$ cm^{-1}. The assignments of some of the fundamental modes and combination bands are given in Table V.

orientations of the intercalant are still possible, viz., with the C_{2v} axis parallel or perpendicular to the van der Waals plane. The molecular diameter of pyridine is estimated to be 4.92 Å parallel to the C_{2v} axis and 5.12 Å perpendicular to this axis in the plane of the ring (i.e., the H_3–H_5 diameter). Since the *b*-axis expansion of FeOCl in forming the pyridine intercalate is 5.54 Å, either orientation could be accommodated in the van der Waals layer, and no clearcut distinction between the two orientations can be drawn from the present data alone. However, two additional observations are pertinent in the present context. Palvadeau et al.[4] have carried out a detailed powder pattern analysis on the intercalates $FeOCl(py)_{1/4}$ and $FeOCl(py)_{1/3}$. In the case of the latter, they note that the a unit cell parameter is doubled, indicating the existence of a super structure in the *a,b* plane. In addition these authors note that ESR data suggest partial transfer of the nitrogen lone-pair electron density into the FeOCl layers. It thus appears clear that a model which is in agreement with these various observations is one in which pyridine molecules form an ordered array within the van der Waals layer, with the lone-pair electrons of the nitrogen aotms of adjacent molecules pointing alternately "up" and "down" toward the iron atoms. It must be emphasized here that these structural inferences apply only to a particular FeOCl intercalate, namely, $FeOCl(py)_{1/3}$. Examination of other intercalants (e.g., 4-(dimethylamino)-pyridine,[5] inter alia) in which the major and minor dimensions within the molecular plane are significantly different or in which ring substituents impose special steric requirements shows that these appear to assume other orientations with respect to the host matrix and must be considered on an individual basis.

$FeOCl(imid)_{1/4}(H_2O)_{1/2}$. The infrared data for this intercalant, using the frequencies reported by Garfinkel and Edsall[21] and the assignments of Cordes and Walter,[22] are summarized in Table VI. Most of the normal modes which involve either ring breathing (expansion) or the CH bending modes and which are prominent features of the spectra reported[21] for imidazole in KCl appear to be either weak or absent in the infrared spectrum of the intrercalate. The prominent normal modes which are observed in the latter are the bands at 620 cm^{-1} (B_2, ν_{21}) due to an NH out-of-plane mode 755 cm^{-1} (B_2, ν_{18}) due to CH out-of-plane bending motions, the band at 1045 cm^{-1} (presumably the A_1, ν_8 mode at 1058 cm^{-1} in the unintercalated base), and the band at 1092 cm^{-1} (B_1, ν_{15}) due to in-plane hydrogen atom scissor motions. In particular, it is significant that the very strong ring-torsional mode at 658 cm^{-1} and the band at 1264 cm^{-1} (A_1, ν_6), assigned to a symmetric ring breathing motion, are completely absent in the intercalate. These data reflect a significant interaction between the heterocyclic ring base and the chlorine atoms of the matrix such that significant nonbonding (Coulomb) interaction must obtain. This conclusion from the vibrational spectral data is particularly interesting in view of the fact that the $FeOCl(imid)_{1/4}(H_2O)_{1/2}$ intercalate Mössbauer spectra show the sigmoid behavior of $QS(T)$, detailed above.

It is clear that a more complete understanding of the chemical interactions between the intercalants and the FeOCl host matrix will require a careful and detailed study by Fourier infrared techniques over a temperature range comparable to that of the Mössbauer spectroscopic data. Such temperature-dependent vibrational spectroscopic studies are currently under way in these laboratories.

Acknowledgment. This research was supported in part by Grant DMR 7808615AO1 from the division of Materials Research, National Science Foundation, the Research Council of Rutgers University, and the Center for Computer and Information Services, Rutgers University. This support is herewith gratefully acknowledged. The authors are also indebted to Dr. M. F. Leahy of RCA Laboratories and to Dr. Alan J. Rein of IBM for assistance with some of the Fourier transform infrared spectra. Helpful discussions with Professor N. B. Koller are also gratefully acknowledged.

Registry No. $FeOCl(py)_{1/3}$, 76613-07-5; $FeOCl(amm)_{3/4}$, 76613-08-6; $FeOCl(isopropyl)_{1/3}$, 76613-09-7; $FeOCl(pic)_{1/4}$, 76613-10-0; $FeOCl(butyl)_{1/4}$, 76613-11-1; $FeOCl(octa)_{1/6}$, 76613-12-2; $FeOCl(imid)_{1/4}$, 76613-13-3; $FeOCl(quin)_{1/6}$, 76613-14-4; $FeOCl(lut)_{1/6}$, 76613-15-5; $FeOCl(dodec)_{1/6}$, 76613-16-6; FeOCl, 13870-10-5; py, 110-86-1.

(21) Garfinkel, D.; Edsall, J. T. *J. Am. Chem. Soc.* **1958**, *80*, 3807.
(22) Cordes de N. D., M.; Walter, J. L. *Spectrochim. Acta, Part A* **1968**, *24A*, 237.

Contribution from Corporate Pioneering Research Laboratories, Exxon Research and Engineering Company, Linden, New Jersey 07036

Ligand Basicity in Complexed Uranyls: Oxygen Bases

G. M. KRAMER,* E. T. MAAS, JR., and M. B. DINES

Received February 20, 1980

The THF adduct of uranyl hexafluoroacetylacetonate undergoes fast reversible displacement reactions with other bases in chloroform solutions. The NMR shift of the α-CH_2 group is found to be a useful monitor of the equilibrium established and has been used to measure the relative strength of oxygenated bases. The values correlate well with Gutmann's donor number (DN), the heat of reaction of the bases with $SbCl_5$.

The THF complex of uranyl hexafluoroacetylacetone (**1**) has recently been shown to be of sufficient stability to sublime intact at temperatures up to 100 °C.[1] This is remarkable in view of the fact that the analogous complex with diethyl ether

